Luminescence

DOI: 10.1002/anie.200704608

Dynamic Control of Photoluminescence for Self-assembled Nanosheet Films Intercalated with Lanthanide Ions by Using a Photoelectrochemical Reaction**

Shintaro Ida, Chikako Ogata, Daisuke Shiga, Kazuyoshi Izawa, Keita Ikeue, and Yasumichi Matsumoto*

Semiconductor oxide nanosheets synthesized by exfoliation of layered oxides are two-dimensional crystals with a thickness of about 1 nm.[1–4] New layered materials and their films can be reassembled by electrostatic self-assembly deposition (ESD)[5] and by layer-by-layer (LBL)[6–8] techniques, respectively. Since the nanosheets have a negative charge in aqueous solution they can be used with various cationic species as the starting materials. Layered materials prepared from nanosheets and lanthanide (Ln) ions are promising as new functional materials because Ln ions have unique properties, such as luminescence and magnetic properties, that are attributable to the 4f electron orbital. For example, the titanate layered oxide intercalated with Eu^{3+} ions prepared from titanate nanosheets and Eu^{3+} ions has unique luminescence properties.[9–11] The layered oxide gives a red emission from the Eu^{3+} ions which is induced by energy transfer through excitation of the bandgap of the titanate nanosheet,[9,10] and the emission from the Eu^{3+} ions is promoted by intercalated water molecules.[10] Furthermore, spectral hole burning caused by the intercalated water molecules was observed in the excitation spectra at room temperature.[11]

Nanosheets of TiO_x, NbO_x, and TaO_x give a high photocurrent during the photoelectrochemical reaction under UV illumination with an energy higher than that of the bandgap.[12] This finding indicates that a large charge separation is produced between the holes in the valence band and the electrons in the conduction band during excitation of the bandgap. Consequently, layered oxide materials intercalated with Ln ions simultaneously exhibit both photoluminescence and a photoelectrochemical reaction during excitation of the bandgap on illumination with UV light. The study reported herein demonstrates a new form of dynamic control over the photoluminescence of Ln ions intercalated in self-assembled nanosheet films of TiO_x and NbO_x. The photoluminescence properties of Ln ions are changed by factors such as a change in the pH value and the addition of anionic species.[13–17] However, it is difficult to dynamically control the photoluminescence properties of Ln^{3+} ions. In the present system, the emission intensities of the intercalated Eu^{3+} and Tb^{3+} ions can be readily controlled by varying the applied potential.

The nanosheet/Ln^{3+} ($Ti_{1.81}O_4$ nanosheet/Eu^{3+} (TiO/Eu) and Nb_6O_{17} nanosheet/Tb^{3+} (NbO/Tb)) films were prepared and fixed on boron-doped diamond electrodes by the LBL technique. The chemical compositions of the TiO/Eu and NbO/Tb films were $Eu_xTi_{1.81}O_4$ ($x = 0.20$–0.30) and $Tb_yNb_6O_{17}$ ($y = 1.30$–1.50), respectively. These are close to the theoretical neutral compositions ($Eu_{0.25}Ti_{1.81}O_4$ and $Tb_{1.33}Nb_6O_{17}$). The Ln^{3+} ions were sandwiched between nanosheets (see Figure S-1 in the Supporting Information). Figure 1 shows a schematic illustration of the system used for the measurement of the photoluminescence. The photoelectrochemical cell with three electrodes, with the nanosheet/Ln^{3+} film acted as a working electrode, was placed in the sample chamber of a fluorescence spectrophotometer. A 0.1 M K_2SO_4 solution (pH 6.5) was used as the electrolyte solution.

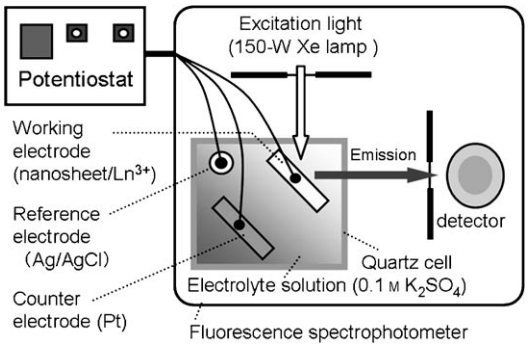

Figure 1. Schematic illustration of the system used for the measurement of the photoluminescence.

Figure 2 shows the emission intensities of the TiO/Eu and NbO/Tb films under illumination by UV light (wavelength: 260 nm) as a function of potential (sweep rate: 20 $mV s^{-1}$). The red emission of the Eu^{3+} ions (614 nm, $^5D_0$-$^7F_2$) appeared in the potential region above about −1.2 V, but disappeared in the potential region below this potential. The same profile was obtained when the emission was monitored at 592 nm ($^5D_0$-$^7F_1$). In the case of the NbO/Tb film, a green emission from the Tb^{3+} ion ($^5D_4$-$^7F_5$) was observed at 545 nm. This

[*] Dr. S. Ida, C. Ogata, D. Shiga, K. Izawa, Dr. K. Ikeue, Prof. Y. Matsumoto
Graduate School of Science and Technology
Kumamoto University
2-39-1 Kurokami, Kumamoto 860-8555 (Japan)
Fax: (+81) 96-342-3679
E-mail: s_ida@chem.kumamoto-u.ac.jp

[**] This work was supported by a Grant-in-Aid for Scientific Research (no. 440, Panoscopic Assembling and High Ordered Functions for Rare Earth Materials, and no. 16080215) from the Ministry of Education, Culture, Sports, Science, and Technology.

Supporting information for this article is available on the WWW under http://www.angewandte.org or from the author.

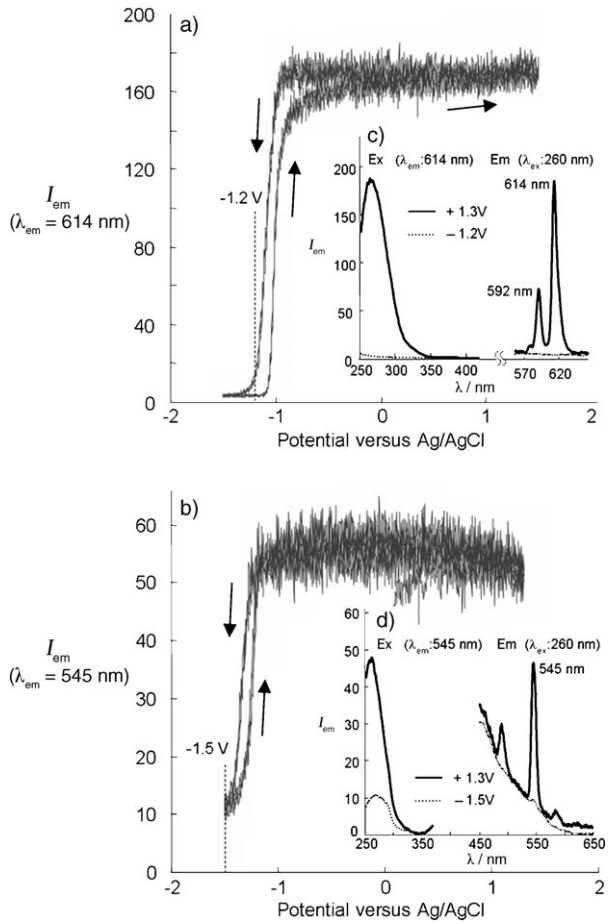

Figure 2. Emission intensity as a function of applied potential (sweep rate: 20 mV min^{-1}) for a) the TiO/Eu film (λ_{ex}: 260 nm, λ_{em}: 614 nm) and b) the NbO/Tb film (λ_{ex}: 260 nm, λ_{em}: 545 nm), as well as photoluminescence spectra recorded at different applied potentials for c) the TiO/Eu film and d) the NbO/Tb film. Em = emission, Ex = excitation.

emission was the strongest of all the emission bands, but disappeared when a potential more negative than about −1.5 V was applied. (The weak emission in the potential region below −1.5 V was due to stray light from the excitation source, as shown in Figure 2b.) Thus, the emission of both the TiO/Eu and NbO/Tb films can be easily controlled by varying the applied potential.

As for the emissions from the TiO/Eu and NbO/Tb films under anodic bias, the excitation spectra showed broad bands in the 250–350 nm range (Figure 2c and d). These were attributed to the bandgap excitation in the nanosheets.[9–11,18–25] The energy released during excitation of the bandgap under UV illumination is transferred to the intercalated Ln^{3+} ions (energy transfer), which induces their specific emissions (Eu^{3+}: red and Tb^{3+}: green). By contrast, no emission was observed in the case of a cathodic bias. As discussed below, this is due to the reduced state of the Ln^{n+} ions (probably $n = 2$) induced by electrons produced in the conduction band of the nanosheet under UV illumination.

The change in emission intensity on varying the electrode potential is due to the photoelectrochemical reduction and oxidation of the intercalated Ln ions. To estimate the flatband potential of the TiO/Eu and NbO/Tb films, the onset potentials of the photoanodic current of the films were measured in a 0.5 M K_2SO_4 solution containing 0.1 M CH_3OH because the onset potential is near to or more positive than the flatband potential. The CH_3OH acts as a sacrificial reagent to capture the holes produced by UV illumination, thus enabling the rising edge of the onset potential to be observed clearly. The onset potentials of the TiO/Eu and NbO/Tb films were about −1.0 and −1.2 V, respectively (see Figure S-2 in the Supporting Information). That is, the flatband potentials are near to or more negative than −1.0 V and −1.2 V for the TiO/Eu and NbO/Tb films, respectively. The potentials bringing about the change in emission are about −1.2 and −1.5 V for the TiO/Eu (Figure 2a) and NbO/Tb (Figure 2b) films, respectively, which agrees with the flatband potentials estimated from the onset potentials of the photoanodic current. In conclusion, the flatband potentials are −1.2 and −1.5 V, respectively, for the TiO/Eu and NbO/Tb films.

A mechanistic model for the change in emission of the nanosheet/Ln^{3+} films is illustrated in Figure 3, where the $Ti_{1.81}O_4$ and Nb_6O_{17} nanosheets act as n-type semiconductors.[12] In the case of cathodic bias (potentials more negative than the flatband potential), an electron generated in the conduction band of the nanosheet by UV illumination at an energy higher than its bandgap moves to the intercalated Ln^{3+} ion, thereby reducing Ln^{3+} to Ln^{n+} (probably $n = 2$), which gives no emission. Actually, the band intensities assigned to the Eu^{2+} species in the XPS spectra of the TiO/Eu film increased after electrolysis at −1.4 V (see Figure S-9 in the Supporting Information), although we could not get evidence for the Tb^{n+} species. In the case of anodic bias (potentials more positive than the flatband potential), a hole produced in the valence band of the nanosheet by UV illumination oxidizes Ln^{n+} to Ln^{3+}. The Ln^{3+} ions then give a specific emission under UV illumination that is based on the energy transfer from the nanosheet to the ions. To confirm the above mechanistic model, the photoluminescence properties of the Eu^{3+} ions in the NbO/Eu film were examined. If only

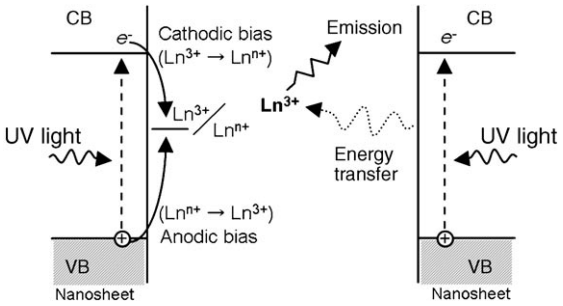

Figure 3. The mechanism for the photoelectrochemical oxidation and reduction of the intercalated Ln ions and the emission attributed to the energy transfer from the nanosheet to the Ln^{3+} ions, where the standard equilibrium potential of Eu^{3+}/Eu^{2+} is about −0.55 V versus Ag/AgCl (see Figure S-8 in theSupporting Information). VB = valence band, CB = conduction band.

the flatband potential of the NbO nanosheet affects the potential that changes the emission intensity (mechanism shown in Figure 3), the latter potential must be the same for both the NbO/Tb and NbO/Eu films because the two samples have the same flatband potential. The potential that changed the emission intensity of the Eu^{3+} ions in the NbO/Eu film was the same as that of the Tb^{3+} ions in the NbO/Tb film (see Figure S-3 in the Supporting Information), but was different from that of Eu^{3+} ions in the TiO/Eu film. These results indicate that the oxidation and reduction of Ln^{3+}/Ln^{2+} in an interlayer of the TiO/Ln and the NbO/Ln films depend on the flatband potential of the nanosheets.

Figure 4 shows the emission intensity of the TiO/Eu film under applied potentials as a function of electrolysis time. A highly reproducible on/off emission was obtained on applying

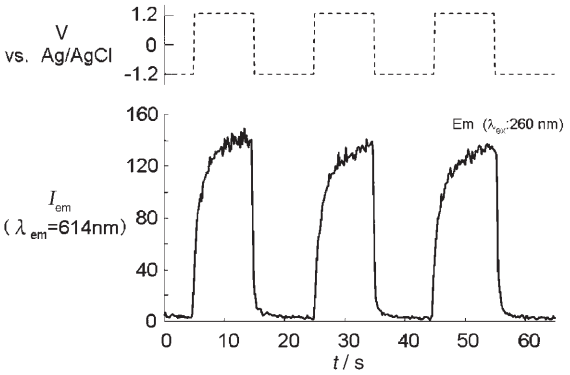

Figure 4. Emission intensity of the TiO/Eu film under an applied pulse potential as a function of electrolysis time.

a pulse potential. The on/off emission was also obtained under a chopping wave potential (see Figure S-4 in the Supporting Information). Thus, the emission from nanosheet films intercalated with Ln^{3+} ions can be controlled by varying the applied potential. The on/off emission response was stable even after 24 h of operation (See Figure S-5 in the Supporting Information).

In conclusion, we have clearly demonstrated an on/off control for the photoluminescence of Eu^{3+} and Tb^{3+} ions in oxide nanosheet/Ln^{3+} films by a mechanism that combines photoelectrochemical oxidation/reduction reactions and energy transfer from the nanosheets to the Ln^{3+} ions. It is anticipated that this dynamic luminescent control system will be useful for electrooptical devises in the near future.

Experimental Section

As the starting materials for the nanosheets, $Cs_xTi_{(2-x/4)}\,\square_{x/4}O_4$ (□: vacancy) and $K_4Nb_6O_{17}$ were prepared.[3,10] $K_4Nb_6O_{17}$ was prepared by heat treatment of a stoichiometric mixture of Nb_2O_5 (8.086 g) and K_2CO_3 (2.806 g) at 1200 °C for 15 min in a Pt crucible. $Cs_xTi_{(2-x/4)}\square_{x/4}O_4$ was prepared by the complex polymerization method.[10] Prior to the addition of $Ti(OCH(CH_3)_2)_4$ (10.796 mL), Cs_2CO_3 (3.4983 g) was dissolved in a mixture of methanol (160 mL) and ethylene glycol (60 mL). During the addition of titanium isopropoxide, the mixture was stirred vigorously with a magnetic stirrer and the temperature was raised gradually to 50 °C. Anhydrous citric acid (28.8 g) was then added and the temperature was raised to 150 °C to yield a resinlike mass, which transformed into ash and then into white powder upon raising the temperature to 300 °C. Heat treatment of the powder at 800 °C yielded the final product. These powders (1 g) were treated with 5 M HNO_3 or 1 M HCl aqueous solution (300 mL) to protonate the interlayer by an ion-exchange reaction between interlayer cations and protons in solution. The protonated powders (0.5 g) were exfoliated in tetrabutylammonium (TBA) solution (300 mL) for 72 h. The amount of TBA in the solution was eightfold higher than that of the powder in terms of the molar ratio. Subsequent centrifugation of the solution under 3000 rpm for 30 min yielded a colloidal suspension of the nanosheets. The host nanosheets obtained from $Cs_xTi_{(2-x/4)}\square_{x/4}O_4$ and $K_4Nb_6O_{17}$ are denoted as $Ti_{1.81}O_4$ nanosheet and Nb_6O_{17} nanosheet, respectively. Deposition of the films by the LBL method was carried out by the same procedure as reported in other related studies,[6–8,10,25] where 0.01 M $Eu(CH_3COO)_3$ (5 mL) and $Tb(CH_3COO)_3$ (5 mL) were used as the cation solutions. A boron-doped diamond electrode (HOKUTO DENKO Corp) was used as a substrate. The substrates were primed in the aqueous solution (5 mL) of poly(ethyleneimine) (PEI, 2.5 g L^{-1}) for 15 min to positively charge the surface of the substrate. Primed substrates were dipped into the nanosheet solution containing negatively charged nanosheets for 15 min, then into the 0.01 M $Eu(CH_3COO)_3$ or the $Tb(CH_3COO)_3$ solution for another 15 min, and finally into the nanosheet solution to form the layered structure of nanosheet/rare earth ions/nanosheet/substrate (nanosheet/Ln^{3+} film). The substrate was rinsed with water to remove the excess adsorbed species between the deposition steps. The chemical compositions of the prepared films were estimated by induction-coupled plasma (ICP) analysis, where the films were dissolved in a mixed solution of concentrated HNO_3 and HF before measurement. Excitation and emission spectra were recorded on a Jasco FP-6500 spectrofluorometer with a 150-W Xe lamp source. All electrochemical experiments were carried out in a conventional three-electrode electrochemical cell with a Pt counter electrode and a saturated Ag/AgCl reference electrode. The photoluminescence (PL) efficiencies of the colloidal solutions of the TiO/Eu and NbO/Tb powders were estimated by comparison with solutions of quinine in aqueous 0.5 M H_2SO_4 (PL efficiency: 54.6 %).[26] The PL efficiencies of the colloidal solutions of the TiO/Eu and NbO/Tb powders at 260 nm were 0.495 and 0.03 %, respectively. The TiO/Eu and Tb/NbO powders were prepared by the ESD method.[10] Since the layered structures and the chemical compositions of the TiO/Eu and NbO/Tb powders are almost the same as those of the TiO/Eu and NbO/Tb films, the estimated PL efficiencies must be close to those of TiO/Eu and NbO/Tb films.

Received: October 5, 2007
Revised: January 8, 2008
Published online: February 18, 2008

Keywords: electrochemistry · layered compounds · luminescence · nanostructures · rare earth metals

[1] T. Sasaki, M. Watanabe, H. Hashizume, H. Yamada, H. Nakazawa, *J. Am. Chem. Soc.* **1996**, *118*, 8329 – 8335.
[2] R. E. Schaak, T. E. Mallouk, *Chem. Mater.* **2000**, *12*, 2513 – 2516.
[3] A. Kudo, A. Tanaka, K. Domen, K. Maruya, K. Aika, T. Onishi, *J. Catal.* **1988**, *111*, 67 – 76.
[4] S. Ida, C. Ogata, U. Unal, K. Izawa, T. Inoue, O. Altuntasoglu, Y. Matsumoto, *J. Am. Chem. Soc.* **2007**, *129*, 8956 – 8957.
[5] U. Unal, Y. Matsumoto, N. Tanaka, Y. Kimura, N. Tamoto, *J. Phys. Chem. B* **2003**, *107*, 12680 – 12689.
[6] M. Fang, D. M. Kaschak, A. C. Sutorik, T. E. Mallouk, *J. Am. Chem. Soc.* **1997**, *119*, 12184 – 12191.
[7] Y. Zhou, R. Ma, Y. Ebina, K. Takada, T. Sasaki, *Chem. Mater.* **2006**, *18*, 1235 – 1239.

[8] T. Sasaki, Y. Ebina, M. Watanabe, G. Decher, *Chem. Commun.* **2000**, 2163 – 2164.
[9] H. Xin, R. Ma, L. Wang, Y. Ebina, K. Takada, T. Sasaki, *Appl. Phys. Lett.* **2004**, *85*, 4187 – 4189.
[10] Y. Matsumoto, U. Unal, Y. Kimura, S. Ohashi, K. Izawa, *J. Phys. Chem. B* **2005**, *109*, 12748 – 12754.
[11] S. Ida, U. Unal, K. Izawa, O. Altuntasoglu, C. Ogata, T. Inoue, K. Shimogawa, Y. Matsumoto, *J. Phys. Chem. B* **2006**, *110*, 23881 – 23887.
[12] K. Izawa, T. Yamada, U. Unal, S. Ida, O. Altuntasoglu, M. Koinuma, Y. Matsumoto, *J. Phys. Chem. B* **2006**, *110*, 4645 – 4650.
[13] O. S. Wolfbeis, A. Dürkop, M. Wu, Z. Lin, *Angew. Chem.* **2002**, *114*, 4681 – 4684; *Angew. Chem. Int. Ed.* **2002**, *41*, 4495 – 4498.
[14] T. Yamada, S. Shinoda, H. Tsukube, *Chem. Commun.* **2002**, 1218 – 1219.
[15] S. Blair, M. P. Lowe, C. E. Mathieu, D. Parker, P. K. Senanayake, R. Kataky, *Inorg. Chem.* **2001**, *40,* 5860 – 5867.
[16] B. Song, G. Wang, M. Tan, J. Yuan, *J. Am. Chem. Soc.* **2006**, *128*, 13442-13450.
[17] T. Gunnlaugsson, J. P. Leonard, K. Sene chal, A. J. Harte, *J. Am. Chem. Soc.* **2003**, *125*, 12062-12063.
[18] M. A. Bizeto, V. R. L. Constantino, H. F. Brito, *J. Alloys Compd.* **2000**, *311*, 159 – 168.
[19] A. Conde-Gallardo, M. Garcia-Rocha, I. Hernandez-Calderon, R. Palomino-Merino, *Appl. Phys. Lett.* **2001**, *78*, 3436 – 3438.
[20] K. L. Frindell, M. H. Bartl, A. Popitsch, G. D. Stucky, *Angew. Chem.* **2002**, *114*, 1001 – 1004; *Angew. Chem. Int. Ed.* **2002**, *41*, 959 – 962.
[21] K. L. Frindell, M. H. Bartl, M. R. Robinson, G. C. Bazan, A. Popitsch, G. D. Stucky, *J. Solid State Chem.* **2003**, *172*, 81 – 88.
[22] A. Kudo, E. Kaneko, *Chem. Commun.* **1997**, 349 – 350.
[23] A. Kudo, E. Kaneko, *Microporous Mesoporous Mater.* **1998**, *21*, 615 – 620.
[24] V. R. L. Constantino, M. A. Bizeto, H. F. Brito, *J. Alloys Compd.* **1998**, *278*, 142 – 148.
[25] S. Ida, K. Araki, U. Unal, K. Izawa, O. Altuntasoglu, C. Ogata, Y. Matsumoto, *Chem. Commun.* **2006**, 3619 – 3621.
[26] C. Li, N. Murase, *Langmuir* **2004**, *20*, 1 – 4.

